J|A|C|S
ARTICLES
Published on Web 05/31/2007

Transition-State Variation in Human, Bovine, and *Plasmodium falciparum* Adenosine Deaminases

Minkui Luo, Vipender Singh, Erika A. Taylor, and Vern L. Schramm*

Contribution from the Department of Biochemistry, Albert Einstein College of Medicine, Bronx, New York 10461

Received March 26, 2007; E-mail: vern@aecom.yu.edu

Abstract: Adenosine deaminases (ADAs) from human, bovine, and *Plasmodium falciparum* sources were analyzed by kinetic isotope effects (KIEs) and shown to have distinct but related transition states. Human adenosine deaminase (HsADA) is present in most mammalian cells and is involved in B- and T-cell development. The ADA from *Plasmodium falciparum* (PfADA) is essential in this purine auxotroph, and its inhibition is expected to have therapeutic effects for malaria. Therefore, ADA is of continuing interest for inhibitor design. Stable structural mimics of ADA transition states are powerful inhibitors. Here we report the transition-state structures of PfADA, HsADA, and bovine ADA (BtADA) solved using competitive kinetic isotope effects (KIE) and density functional calculations. Adenines labeled at [6-^{13}C], [6-^{15}N], [6-^{13}C, 6-^{15}N], and [1-^{15}N] were synthesized and enzymatically coupled with [1′-^{14}C] ribose to give isotopically labeled adenosines as ADA substrates for KIE analysis. [6-^{13}C], [6-^{15}N], and [1-^{15}N]adenosines reported intrinsic KIE values of (1.010, 1.011, 1.009), (1.005, 1.005, 1.002), and (1.004, 1.001, 0.995) for PfADA, HsADA, and BtADA, respectively. The differences in intrinsic KIEs reflect structural alterations in the transition states. The [1-^{15}N] KIEs and computational modeling results indicate that PfADA, HsADA, and BtADA adopt early S_NAr transition states, where N1 protonation is partial and the bond order to the attacking hydroxyl nucleophile is nearly complete. The key structural variation among PfADA, HsADA, and BtADA transition states lies in the degree of N1 protonation with the decreased bond lengths of 1.92, 1.55, and 1.28 Å, respectively. Thus, PfADA has the earliest and BtADA has the most developed transition state. This conclusion is consistent with the 20−36-fold increase of k_{cat} in comparing PfADA with HsADA and BtADA.

Introduction

Adenosine deaminase (ADA) catalyzes the irreversible hydrolysis of adenosine or 2′-deoxyadenosine to the corresponding inosine and ammonia (Figure 1). The enzyme has been found in a wide variety of microorganism, plants, invertebrates, and mammals.[1] In humans, it is a key enzyme for lymphoid differentiation, maturation,[1] and activation.[2] Heritable ADA deficiency causes severe combined immunodeficiency disease,[3] whose pathogenesis is caused by high concentration of 2′-dexoyadenosine-5′-triphosphate (dATP).[4,5] Consequently, ADA inhibitors have been therapeutically useful as antimetabolic and antineophastic agents as well as neurological modulators through their effects on adenosine levels.[6−8] Other applications of human ADA (HsADA) inhibitors include their beneficiary effects on myocardial ischemia as protective agents,[9] on leukemia as immunosuppressors,[4] and on lymphoproliferative malignancies by accumulating lymphotoxic dATP.[5,7] *Plasmodium falciparum* is a purine auxotroph, and its ADA (PfADA) is a key enzyme in its purine salvage pathway.[10] Targeting PfADA is therefore a promising approach to treat malaria, a disease responsible for 1 million deaths every year.[10]

A number of ADA inhibitors have been characterized, and they fall into the following categories:[4] (i) substrate-like inhibitors whose structures are similar to adenosine; (ii) transition-state analogue inhibitors that resemble the tetrahedral Meisenheimer intermediate (Figure 1). Erythro-9-(2-hydroxy-3-nonyl)adenine is an example for the former,[11] while coformycin and 2′-dexoycoformycin (pentostatin) are examples of ADA transition-state analogues.[12] Clinical use of the known inhibitors has been limited due to their low chemical stability or high toxicity.[6] Consequently, there is a continued interest in the development of stable and low-toxicity ADA inhibitors.

Transition-state theory proposes that a perfect analogue of an enzymatic transition state can bind the enzyme tighter than

(1) Cristalli, G.; Costanzi, S.; Lambertucci, C.; Lupidi, G.; Vittori, S.; Volpini, R.; Camaioni, E. *Med. Res. Rev.* **2001**, *21*, 105−128.
(2) Kameoka, J.; Tanaka, T.; Nojima, Y.; Schlossman, S. F.; Morimoto, C. *Science* **1993**, *261*, 466−469.
(3) Wilson, D. K.; Rudolph, F. B.; Quiocho, F. A. *Science* **1991**, *252*, 1278−1284.
(4) Da Settimo, F.; Primofiore, G.; La Motta, C.; Taliani, S.; Simorini, F.; Marini, A. M.; Mugnaini, L.; Lavecchia, A.; Novellino, E.; Tuscano, D.; Martini, C. *J. Med. Chem.* **2005**, *48*, 5162−5174.
(5) Cohen, A.; Hirschhorn, R.; Horowitz, S. D.; Rubinstein, A.; Polmar, S. H.; Hong, R.; Martin, D. W., Jr. *Proc. Natl. Acad. Sci. U.S.A.* **1978**, *75*, 472−476.
(6) Kinoshita, T.; Nishio, N.; Nakanishi, I.; Sato, A.; Fujii, T. *Acta Crystallogr., Sect. D* **2003**, *59*, 299−303.
(7) Glazer, R. I. *Cancer. Chemother. Pharmacol.* **1980**, *4*, 227−235.
(8) Centelles, J. J.; Franco, R.; Bozal, J. *J. Neurosci. Res.* **1988**, *19*, 258−267.
(9) Law, W. R. *Cardiovasc. Res.* **2006**, *71*, 8−9.
(10) Ting, L. M.; Shi, W.; Lewandowicz, A.; Singh, V.; Mwakingwe, A.; Birck, M. R.; Taylor Ringia, E. A.; Bench, G.; Madrid, D. C.; Tyler, P. C.; Evans, G. B.; Furneaux, R. H.; Schramm, V. L.; Kim, K. *J. Biol. Chem.* **2005**, *280*, 9547−9554.
(11) Schaeffer, H. J.; Schwender, C. F. *J. Med. Chem.* **1974**, *17*, 6−8.
(12) Wolfenden, R. *Bioorg. Med. Chem.* **1999**, *7*, 647−652.

10.1021/ja072122y CCC: $37.00

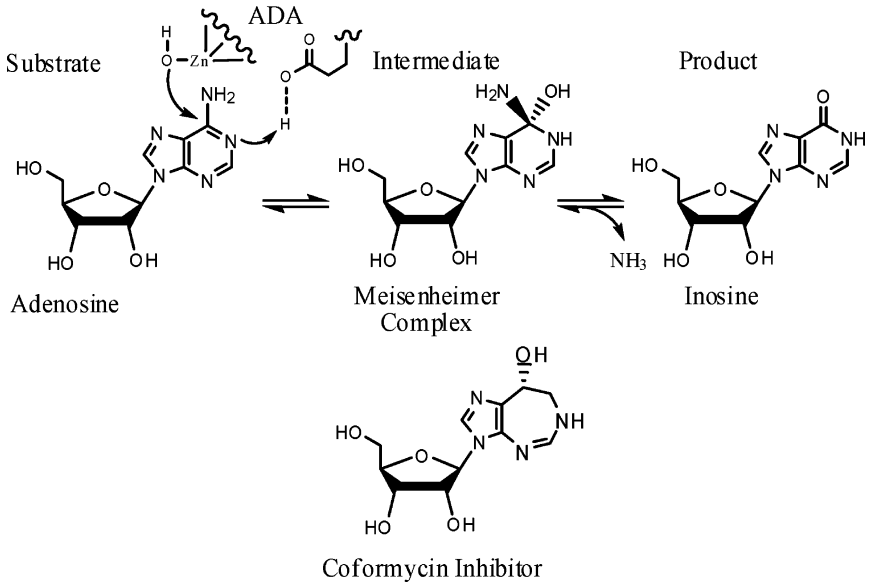

Figure 1. Reaction catalyzed by adenosine deaminases and the structure of *R*-coformycin.

its substrate by a factor equivalent to the catalytic acceleration imposed by the enzyme. For enzymes with K_m values in the micromolar range and catalytic accelerations of $10^{12}-10^{15}$, perfect transition-state analogues are expected to bind with K_d values of $10^{-18}-10^{-21}$ M.[13−17] Therefore, enzymatic transition-state structures provide a blueprint for the design of powerful, target-specific inhibitors. Even enzymes with high sequence homology can have significantly distinct transition states.[18−21] PfADA, HsADA, and BtADA are functionally similar and carry out similar deamination reactions. However, they differ from one another in terms of their catalytic turnover (k_{cat}). For instance, the k_{cat} of 65 s^{-1} for bovine ADA (BtADA) is 36-fold faster than the rate of 1.8 s^{-1} for PfADA. The ADA transition-state analogue coformycin also binds 25-fold more tightly to BtADA than PfADA.[10] In addition, PfADA has a substrate specificity including both 5′-methylthioadenosine and adenosine, while mammalian ADAs do not use 5′-methylthioadenosine as a substrate.[10,22] These unique features of ADAs stimulated us to probe the transition-state structures of the ADA isozymes from *P. falciparum*, human, and bovine sources.

Kinetic isotope effects (KIE) allow experimental access to the transition-state structures of enzymatic reactions and are a powerful tool for obtaining detailed transition-state information.[14,17,23] This method has been used successfully to study the transition states of many *N*-ribosyl transferases.[15,19,24−28] Our interest in enzymatic transition states led us to determine the transition-state structures of PfADA, HsADA, and BtADA via the KIE approach. We also report a new synthetic method for making [6-^{13}C]-, [6-^{15}N]-, and [6-^{13}C, 6-^{15}N]-labeled adenines. These adenines, together with [1-^{15}N] adenine, were combined with [1′-^{14}C] or [1′-^{3}H] riboses to give isotopically labeled adenosines as substrates. The set of KIEs for the three ADAs were determined under competitive conditions. The intrinsic [1-^{15}N], [6-^{13}C], and [6-^{15}N] KIEs and density functional calculations propose early transition states close to the Meisenheimer intermediate for PfADA, HsADA, and BtADA. The key structural variation among the three ADAs lies in the degree of N1 protonation with an increased N1−H Pauling bond order of 0.05 for PfADA, 0.16 for HsADA, and 0.42 for BtADA. Thus, PfADA has the earliest and BtADA has the transition state most similar to the tetrahedral Meisenheimer intermediate. Protonation of NH_2-6 and subsequent deamination are therefore proposed to occur after the rate-limiting formation of the Meisenheimer intermediate. This conclusion is consistent with the observed 20−36-fold increase of k_{cat} in comparing PfADA with HsADA and BtADA.[10,22,29]

Experimental Section

Reagents and Materials. The [1′-^{3}H]- and [1′-^{14}C]riboses were purchased from American Radiolabeled Chemicals Inc. Isotopically labeled potassium cyanides (K^{13}CN, KC^{15}N, K^{13}C^{15}N) were obtained from Aldrich. [1-^{15}N]Adenine was synthesized according to the reported procedures.[30] Adenylate kinase (AK), pyruvate kinase (PK), hexokinase, and bovine spleen adenosine deaminase (BtADA) were purchased from Sigma. Phospho-D-ribosyl-1-pyrophosphate (PRPP) synthase and adenine phosphoribosyltransferase (APRTase) were purified according to the methods reported previously.[31,32] Alkaline phosphatase was purchased from Roche. Ribokinase (RK) was obtained as described

(13) Wolfenden, R.; Snider, M. J. *Acc. Chem. Res.* **2001**, *34*, 938−945.
(14) Schramm, V. L. *Arch. Biochem. Biophys.* **2005**, *433*, 13−26.
(15) Schramm, V. L. *Curr. Opin. Struct. Biol.* **2005**, *15*, 604−613.
(16) Schramm, V. L. *Acc. Chem. Res.* **2003**, *36*, 588−596.
(17) Schramm, V. L. *Methods Enzymol.* **1999**, *308*, 301−355.
(18) Taylor Ringia, E. A.; Tyler, P. C.; Evans, G. B.; Furneaux, R. H.; Murkin, A. S.; Schramm, V. L. *J. Am. Chem. Soc.* **2006**, *128*, 7126−7127.
(19) Lewandowicz, A.; Schramm, V. L. *Biochemistry* **2004**, *43*, 1458−1468.
(20) Lewandowicz, A.; Taylor Ringia, E. A.; Ting, L. M.; Kim, K.; Tyler, P. C.; Evans, G. B.; Zubkova, O. V.; Mee, S.; Painter, G. F.; Lenz, D. H.; Furneaux, R. H.; Schramm, V. L. *J. Biol. Chem.* **2005**, *280*, 30320−30328.
(21) Kline, P. C.; Schramm, V. L. *Biochemistry* **1993**, *32*, 13212−13219.
(22) Tyler, P. C.; Taylor, E. A.; Fröhlich, R. F. G.; Schramm, V. L. *J. Am. Chem. Soc.* **2007**, *129*, 6872−6879.
(23) Cleland, W. W. *Arch. Biochem. Biophys.* **2005**, *433*, 2−12.
(24) Singh, V.; Schramm, V. L. *J. Am. Chem. Soc.* **2007**, *129*, 2783−2795.
(25) Singh, V.; Schramm, V. L. *J. Am. Chem. Soc.* **2006**, *128*, 14691−14696.
(26) Talyor Ringia, E. A.; Schramm, V. L. *Curr. Top. Med. Chem.* **2005**, *5*, 1237−1258.
(27) Singh, V.; Lee, J. E.; Nunez, S.; Howell, P. L.; Schramm, V. L. *Biochemistry* **2005**, *44*, 11647−11659.
(28) Birck, M. R.; Schramm, V. L. *J. Am. Chem. Soc.* **2004**, *126*, 2447−2453.
(29) Kurz, L. C.; Moix, L.; Riley, M. C.; Frieden, C. *Biochemistry* **1992**, *31*, 39−48.
(30) Sethi, S. K.; Gupta, S. P.; Jenkins, E. E.; Whitehead, C. W.; Townsend, L. B.; McCloskey, J. A. *J. Am. Chem. Soc.* **1982**, *104*, 3349−3353.
(31) Merkler, D. J.; Kline, P. C.; Weiss, P.; Schramm, V. L. *Biochemistry* **1993**, *32*, 12993−13001.
(32) Shi, W.; Tanaka, K. S.; Crother, T. R.; Taylor, M. W.; Almo, S. C.; Schramm, V. L. *Biochemistry* **2001**, *40*, 10800−10809.

previously.[31,33] HsADA was purchased from Sigma or was a generous gift of Dr. Kami Kim and Li-Min Ting (Department of Microbiology and Immunology at Albert Einstein College of Medicine). PfADA was prepared as described previously.[22] All other reagents were obtained from readily available commercial sources and used without further purification.

Synthesis. General Methods. All reagents and solvents were purchased from commercially available sources and used without further purification. Proton nuclear magnetic resonance (^{1}H NMR), carbon nuclear magnetic resonance (^{13}C NMR), and nitrogen nuclear magnetic resonance (^{15}N NMR) were recorded in CD_3OD or DMSO-d_6 using a Bruker 300 MHz instrument. 1-D ^{13}C and ^{15}N NMR spectra were collected using continuous proton-decoupling mode with at least 10 000 scans. Proton chemical shifts were referenced to internal 3-(trimethylsilyl)propionate. ^{15}N and ^{13}C chemical shifts were referenced indirectly from the proton chemical shift reference. Electrospray ionization (ESI) mass spectra were determined on LCQ LC/MS^n (Finnigan Corp.) using either positive or negative modes.

[4-^{13}C]-, [4-^{15}N]-, and [4-^{13}C, 4-^{15}N]-5-Nitro-1-(tetrahydropyran-2-yl)imidazolecarbonitriles 3. [4-^{13}C]-, [4-^{15}N]-, and [4-^{13}C, 4-^{15}N]-labeled **3** were prepared according to the method described previously.[34] Briefly, [4-^{13}C]-, [4-^{15}N]-, and [4-^{13}C, 4-^{15}N]-5-nitroimidazolecarbonitriles **2** (420 mg, 3 mmol),[35] 3,4-dihydro-2*H*-pyran (0.563 mL, 6 mmol), and *p*-TsOH (15 mg) were added into 6 mL of EtOAc, and the reaction mixture was stirred at room temperature for 2 h. Triethylamine (TEA, 0.02 mL) and hexane (9 mL) were added, and the supernatant was subject to a short silica column. The impurities were eluted with 40% EtOAc/hexane, followed by the elution of [4-^{13}C]-, [4-^{15}N]-, and [4-^{13}C, 4-^{15}N]-labeled **3** with 80% EtOAc/hexane. The solvents were removed in vacuo to give 0.63−0.65 g of ^{13}C/^{15}N/^{13}C^{15}N-labeled products with yield 96−98%. [4-^{13}C]-, [4-^{15}N]-, and [4-^{13}C, 4-^{15}N]-labeled **3**: ^{1}H NMR (300 Hz, CD_3OD) δ ppm 8.18 (s, 1H, N═CH−N), 5.56 (dd, 1H, O−CH−N), 4.12 (m, 1H, O−CH_2−C), 3.81 (m, 1H, O−CH_2−C), 1.7−2.3 (m, 6H, C−CH_2−C); ^{13}C NMR (75 Hz, CD_3OD) δ ppm 153.2, 139.7, 109.2 (CN, singlet for ^{13}C and ^{15}N and doublet for ^{13}C^{15}N), 102.5 (singlet for ^{15}N and doublet for ^{13}C and ^{13}C^{15}N), 88.2, 70.1, 32.3, 26.6, 23.5. [4-^{15}N]- and [4-^{13}C, 4-^{15}N]-labeled **3**: ^{15}N NMR (75 Hz, CD_3OD) δ ppm 284 (singlet for ^{15}N and doublet for ^{13}C^{15}N).

[4-^{13}C]-, [4-^{15}N]-, and [4-^{13}C,4-^{15}N]-5-Amino-1-(tetrahydropyran-2-yl)imidazolecarbonitriles 4. A mixture of [4-^{13}C]-, [4-^{15}N]-, and [4-^{13}C, 4-^{15}N]-5-nitro-1-(tetrahydropyran-2-yl)imidazole-carbonitriles **3** (446 mg, 2 mmol) and 160 mg of Raney nickel in 20 mL of EtOH−H_2O (95:5) was stirred under 1 atm H_2 at room temperature for 16 h. The disappearance of **3** and formation of **4** were confirmed by thin layer chromatography (TLC) using 80% EtOAc−hexane and 10% MeOH−$CHCl_3$ as developing solvents, respectively. The reaction mixture was then passed through a 3-cm self-packed Celite 521 column. The volatile residues of the filtrate were removed under reduced pressure, followed by oil pump vacuum for overnight to give **4** (375−380 mg, 97−98% yield). [4-^{13}C]-, [4-^{15}N]-, and [4-^{13}C, 4-^{15}N]-labeled **4**: ^{1}H NMR (300 Hz, CD_3OD) δ ppm 7.60 (s, 1H, N═CH−N), 5.25 (dd, 1H, O−CH−N), 4.07 (m, 1H, O−CH_2−C), 3.69 (m, 1H, O−CH_2−C), 1.7−2.3 (m, 6H, C−CH_2−C); ^{13}C NMR (75 Hz, CD_3OD) δ ppm 158.8, 137.6, 113.4 (CN, singlet for ^{13}C and doublet for ^{13}C^{15}N and ^{15}N), 84.5, 83.2 (singlet for ^{15}N and doublet for ^{13}C and ^{13}C^{15}N), 68.8, 32.3, 26.6, 23.5. [4-^{15}N]- and [4-^{13}C, 4-^{15}N]-labeled **4**: ^{15}N NMR (75 Hz, CD_3OD) δ ppm 284 (singlet for ^{15}N and doublet for ^{13}C^{15}N); ESI MS (*m*/*e*) std $C_9H_{14}N_4O$ (M + 1) 192.80, found 193.80 for $^{13}C_1C_8H_{13}N_4O$, 193.73 for $C_9H_{13}{}^{15}N_1N_3O$, 194.89 for $^{13}C_1C_8H_{13}{}^{15}N_1N_3O$.

[4-^{13}C]-, [4-^{15}N]-, and [4-^{13}C, 4-^{15}N]-5-Amino-1*H*-imidazolecarbonitrile (5a,b). Compound **4** (195 mg, 1 mmol) was dissolved in TFA−MeOH (14 mL, 2:5), and the solution was stirred for 14 h. Complete conversion from **4** to **5** was confirmed by TLC using 20% MeOH−$CHCl_3$ as the developing solvent. 3,4-Dihydro-*2H*-pyran, TFA, and MeOH in the reaction mixture were removed by reduced pressure, followed by overnight oil pump vacuum to give **5a** + **5b** quantitively. The ratio of **5a**,**b** is around 9:1, the latter of which was generated through the migration of 3,4-dihydro-*2H*-pyran to 5-amino group of **5a** under acidic conditions. However, this mixture was not subject to further purification because the THP group was readily removed in the subsequent cyclization step. [4-^{13}C]-, [4-^{15}N]-, and [4-^{13}C, 4-^{15}N]-labeled **5a**: ^{1}H NMR (300 Hz, CD_3OD) δ ppm 8.04 (s, 1H, N═CH−N). 4-^{13}C/^{13}C^{15}N-labeled **5a**: ^{13}C NMR (75 Hz, CD_3OD) δ ppm 111.8 (CN, singlet for ^{13}C and doublet for ^{13}C^{15}N). [4-^{13}C]-, [4-^{15}N]-, and [4-^{13}C, 4-^{15}N]-labeled **5a**: ^{15}N NMR (75 Hz, CD_3OD) δ ppm 272 (singlet for ^{15}N and doublet for ^{13}C^{15}N); ESI MS (*m*/*e*) std $C_4H_5N_4$ (M + 1) 109.13, found 110.13 for $^{13}C_1C_3H_5N_4$, 110.13 for $C_4H_5{}^{15}N_1N_3$, 111.13 for $^{13}C_1C_3H_5{}^{15}N_1N_3$. [4-^{13}C]-, [4-^{15}N]-, and [4-^{13}C, 4-^{15}N]-labeled **5b**: ^{1}H NMR (300 Hz, CD_3OD) δ ppm 7.73 (s, 1H, N═CH−N), 4.74 (m, 1H, O−CH−N), 3.94 (m, 1H, O−CH_2−C), 3.68 (m, 1H, O−CH_2−C), 1.7−2.3 (m, 6H, C−CH_2−C). [4-^{13}C]- and [^{13}C^{15}N]-labeled **5b**: ^{13}C NMR (75 Hz, CD_3OD) δ ppm 113.6 (CN, singlet for ^{13}C and doublet for ^{13}C^{15}N). [4-^{15}N]- and [4-^{13}C, 4-^{15}N]-labeled **5b**: ^{15}N NMR (75 Hz, CD_3OD) δ ppm 266 (singlet for ^{15}N and doublet for ^{13}C^{15}N).

[6-^{13}C], [6-^{15}N], and [6-^{13}C, 6-^{15}N]Adenines 6. TEA (1.3 mL, 10 mmol) was added into 10 mL of 2-ethoxyethanol containing 9:1 **5a**,**b** (120 mg, 1 mmol) and formamidine acetate (440 mg, 4 mmol). All solids were dissolved when the reaction was heated to 90 °C. The reaction mixture was then stirred under these conditions for another 12 h, and volatile residues were removed under reduced pressure, followed by oil pump vacuum for 24 h. The solid residues were subject to recrystallization in hot water to give pure [6-^{13}C], [6-^{15}N], and [6-^{13}C, 6-^{15}N]adenines (125−135 mg, 90−98%). [6-^{13}C]-labeled adenine **6**: ^{1}H NMR (300 Hz, CD_3OD) δ ppm 8.19 (d, 1H, 2 position), 8.10 (s, 1H, 8 position); ^{13}C NMR (75 Hz, CD_3OD) δ ppm 156.4 (s, ^{13}CN); ESI MS (*m*/*e*) std $C_5H_8N_5$ (M − 1) 136.13, found 137.13 for $^{13}C_1C_4H_8N_5$. [6-^{15}N]-labeled adenine **6**: ^{1}H NMR (300 Hz, CD_3OD) δ ppm 8.19 (s, 1H, 2-H), 8.10 (s, 1H, 8-H); ^{15}N NMR (75 Hz, DMSO-d_6) δ ppm 82 (s, C^{15}N); ESI MS (*m*/*e*) std $C_5H_8N_5$ (M − 1) 136.13, found 137.13 for $C_5H_8{}^{15}N_1N_4$. [6-^{13}C, 6-^{15}N]adenine **6**: ^{1}H NMR (300 Hz, CD_3OD) δ ppm 8.19 (d, 1H, 2 position), 8.10 (s, 1H, 8 position); ^{13}C NMR (75 Hz, CD_3OD) δ ppm 156.4 (d, ^{13}C^{15}N); ^{15}N NMR (75 Hz, DMSO-d_6) δ ppm 82 (d, ^{13}C^{15}N); ESI MS (*m*/*e*) std $C_5H_8N_5$ (M − 1) 136.13, found 138.13 for $^{13}C_1C_4H_8{}^{15}N_1N_4$.

Synthesis of Isotopically Labeled Adenosines. [6-^{13}C]-, [6-^{15}N]-, [6-^{13}C, 6-^{15}N]-, [1-^{15}N]-, [1′-^{3}H]-, and [1′-^{14}C]-labeled adenosines were prepared from radiolabeled riboses **7** and isotopically labeled adenines through two one-pot enzymatic reactions. Specifically labeled ATPs were synthesized as described previously with some modification.[33] Here ribose was used as a starting material instead of glucose. Radiolabeled ribose 5-phosphate was generated by ribokinase (RK). Briefly, 2 mM adenine and 1 mM ribose (final concentrations) were added into a solution containing 20 mM phosphoenolpyruvate, 0.1 mM ATP, 100 mM phosphate, 50 mM glycylglycine, 50 mM KCl, 20 mM $MgCl_2$, and 2 mM DTT (pH = 7.4). The reaction was initialized by the addition of an enzyme stock containing 0.01 unit of ribokinase, 0.01 unit of adenine phosphoribosyltransferase, 0.01 unit of phospho-D-ribosyl-1-pyrophosphate synthase, 1 unit of adenylate kinase, and 1 unit of pyruvate kinase. The reaction mixture was incubated at 30 °C for 12 h to generate radiolabeled ATPs and then heated to 95 °C for 3 min. Into this solution 5 mM glucose, 4 units of hexokinase, 5 units of adenylate kinase, and 10 units of alkaline phosphatase were added. The reaction mixture was incubated at 30 °C for 10 h to allow the conversion of ATP to adenosine. The conversion from ATP to adenosine is slow in the presence of only alkaline phosphatase, probably due to

(33) Parkin, D. W.; Leung, H. B.; Schramm, V. L. *J. Biol. Chem.* **1984**, *259*, 9411−9417.
(34) Wanner, M. J.; Koomen, G. J. *J. Chem. Soc., Perkin Trans. 1* **2002**, 1877−1880.
(35) Suwinski, J.; Swierczek, K. *J. Labelled Compd. Radiopharm.* **2002**, *45*, 795−801.

the less optimized condition (pH = 7.4) for this enzyme. Consequently, the three enzymatic transformations were used for rapid conversion of ATP to adenosine under current conditions. Isotopically labeled adenosines **12a**−**f** were purified by reverse phase HPLC (C-18 Deltapak column, 7.5% MeOH−H_2O, 1 mL/min). The peak eluting at 260 nm corresponded to adenosine (retention time, 14 min). Solvent was removed by speedvac to give adenosines with 98% yield on the basis of the conversion from adenines. The purities of **12a**−**f** were confirmed by comparing the ESI MS, UV spectral profile, and HPLC retention time with authentic adenosine. Stock solutions of 1 mM adenosines **12a**−**f** were prepared and stored at −20 °C before use.

Determination of KIEs by Isotope Ratio Analysis. All ADA-catalyzed deamination reactions were carried out at 25 °C in a buffer containing 20 mM phosphate and 1 μM EDTA (pH = 7.0) unless indicated otherwise. KIEs were determined by the competitive radiolabeled method described previously.[17,25,27,28] Briefly,$^{13}(V_{max}/K_m)$,$^{15}(V_{max}/K_m)$, and $^{13,15}(V_{max}/K_m)$ of PfADA, HsADA, and BtADA were measured using the radiolabeled adenosines containing [6-^{13}C, 1′-^{14}C]-, [6-^{15}N, 1′-^{14}C]-, [6-^{13}C, 6-^{15}N, 1′-^{14}C]-, or [1-^{15}N, 1′-^{14}C]adenosines as the isotope-labeled reactants and [1′-^{3}H]adenosine as the remote label. Each assay was performed in a total volume of 1 mL containing 1 nM ADA and 250 μM substrate (at least 10^5 cpm for ^{14}C and 3:1 for ^{3}H:^{14}C cpm). Reactions were allowed to proceed to 20−30% completion and split into three aliquots. The reaction of one aliquot was allowed to reach 100% completion by adding another 5 nM enzyme, while the other two were quenched by heating to 95 °C for 3 min. All samples were resolved by reverse phase HPLC (C-18 Deltapak column, 50 mM TEA/HOAc, pH = 5.0, 1 mL/min). The fractions containing inosine product were collected, dried by speedvac, and dissolved in 200 μL H_2O, followed by the addition of 20 mL of liquid scintillation counter cocktail (Ultima Gold). The samples were counted for 6 cycles at 10 min/cycle (Wallac 1414 LSC, Perkin-Elmer) and averaged. At least five duplicates were performed for each KIE measurement.

^{3}H and ^{14}C emissions for each sample were determined according to eqs 1 and 2. The ^{14}C channel ratio was obtained by counting a 1′-^{14}C-inosine standard to determine the ratio between channel A and channel B. Channel A and B were set such that all ^{3}H counts appear in channel A and only ^{14}C counts appear in channel B.

$$\text{cpm}(^3\text{H}) = \text{cpm}_{\text{channelA}} - \text{cpm}_{\text{channelB}} \times (^{14}\text{C channel ratio}) \quad (1)$$

$$\text{cpm}(^{14}\text{C}) = \text{cpm}_{\text{channelB}} \times (1 + {}^{14}\text{C channel ratio}) \quad (2)$$

The ^{3}H:^{14}C ratio was determined for the partial and complete reactions, and the KIEs were corrected for 0% reaction according to eq 3, where f is the fraction of reaction completion and R_f and R_0 are the ratios of heavy to light isotope at partial and 100% completion of reaction, respectively.

$$\text{KIE} = \frac{\ln(1-f)}{\ln\left[1 - f\left(\frac{R_f}{R_0}\right)\right]} \quad (3)$$

Measurement of Forward Commitment Factors. Forward commitment factors of the three ADAs were determined by isotope trapping under rapid-mixing pre-steady-state conditions.[27] Briefly, 25.1 μL of stock solution of PfADA (60 μM), HsADA (62.2 μM), or BtADA (60 μM) was mixed with 20.9 μL of 320 μM [1′-^{3}H]adenosine (total 5.5 × 10^5 cpm) for 2 ms using a quench flow apparatus (PQF-3, KinTek). A chase solution containing 10−20 mM adenosine, 20 mM phosphate, and 1 μM EDTA (pH = 7.0) was added rapidly through the third syringe to the final volume of 1 mL with an unlabeled adenosine excess of 1500−3000. Subsequently, 100 μL of aliquots was collected every 15 s for 2.5 min and quenched with 50 μL of 1 N HCl for 3 min, followed by neutralization with 50 μL of 1 N KOH. The [1′-^{3}H]inosine product was purified through reverse phase HPLC and analyzed by scintillation counting as described above. The amount of [1′-^{3}H]inosine generated after the chase step was corrected for background counting, and the [1′-^{3}H]inosine generated during mixing, calculated on the basis of k_{cat},[22] concentrations of the enzymes, and the mixing times. The amount of ADA-bound [1′-^{3}H]adenosine prior to the chase step was calculated on the basis of K_m and the concentrations of the ADAs and [1′-^{3}H]adenosine.[22] The ratios of [1′-^{3}H]inosine product to ADA-bound [1′-^{3}H]adenosine were plotted vs time t (Figure 2). The forward commitment factors C_f for PfADA, HsADA, and BtADA were obtained from the ordinate intercepts upon extrapolation to zero time (forward commitment = intercept/(1 − intercept)).

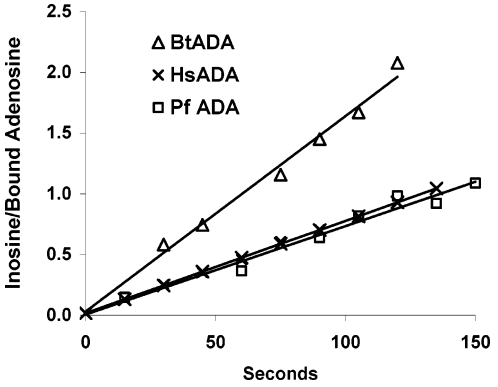

Figure 2. Measurement of forward commitment factors of PfADA, HsADA, and BtADA. The isotope trapping experiments for measuring the forward commitment for PfADA, HsADA, and BtADA were performed under rapid-mixing pre-steady-state conditions. Enzymes were bound to [1′-^{3}H]adenosine in a 2 ms mix and were diluted into a large excess of unlabeled cold adenosine. The ratios of [1′-^{3}H]inosine to enzyme-bound [1′-^{3}H]adenosine were plotted vs time. The forward commitment factors (C_f) for PfADA, HsADA, and BtADA were calculated from the ordinate intercepts, fit to a linear equation. C_f values of 0.006 ± 0.001, 0.020 ± 0.004, and 0.03 ± 0.005 were obtained for PfADA, HsADA, and BtADA, respectively.

Computational Modeling of the Transition States. The transition states of PfADA, HsADA, and BtADA were determined in vacuo using hybrid density functional methods implemented in Gaussian 98.[36] 9-Methyladenine was used as a substrate mimic, and a hydroxyl anion, as the nucleophile. The structures of adenosine, the unconstrained transition state, Meisenheimer intermediate, inosine, and coformycin were optimized using the B3LYP functional and the 6-31G (d, p) basis set. For these calculations the ribosyl moieties were replaced by a methyl group in both modeling and structural display. Bond frequencies for the substrate, transition state, and Meisenheimer intermediate were calculated using the same level of theory. All $3N - 6$ vibrational modes were used for calculating kinetic isotope effects using the ISOEFF98 program.[37] Frequencies of the substrate, the transition state, and a reaction-coordinate imaginary frequency of 50i cm^{-1} or greater were used as the inputs. The KIEs calculated by this procedure were compared with the intrinsic KIEs for additional optimization of the transition states. The initial transition-state structure was generated without imposing any constraints and represents the saddle point for the in vacuo reaction coordinate. A single imaginary frequency of 286i cm^{-1} was obtained and corresponds to the reaction coordinate.

The [1-^{15}N], [6-^{13}C], and [6-^{15}N] KIEs of PfADA, HsADA, and BtADA were used as the constraints to establish the transition states. The optimization process started with computed equilibrium isotope effects from the fully formed Meisenheimer complex. Transition-state structures (Figure 3) were obtained by systematically altering [C6−N6], [C6−$O^{hydroxyl}$], [C6−N1], and [N1−H] bond distances in point calculations with Gaussian. Here we used the equilibrium isotope effects (EIEs) for comparison with the experimental KIEs.[25] The certainty of

(36) Frisch, M. J.; et. al. *Gaussian 98*; Gaussian, Inc.: Pittsburgh, PA, 1998 (complete reference in Supporting Information).
(37) Anisimov, V.; Paneth, P. *J. Math. Chem.* **1999**, *26*, 75−86.

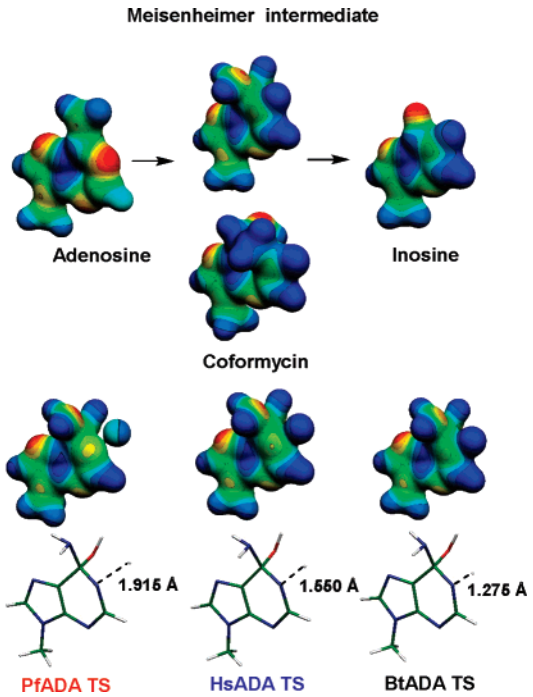

Figure 3. Structures and MEPs of PfADA, HsADA, and BtADA transition states (TS), adenosine, the Meisenheimer intermediate, inosine, and coformycin. The transition states of PfADA, HsADA, and BtADA were determined in vacuo using the hybrid density functional method implemented in Gaussian 98 using the B3LYP functional and 6-31G (d, p) basis set. The [1-^{15}N], [6-^{13}C], and [6-^{15}N] KIEs of PfADA, HsADA, and BtADA were used as the constraints to optimize the transition-state structures. The energy-minimum structures of adenosine, the Meisenheimer intermediate, inosine, and coformycin were obtained with the same computational parameters. The CUBE subprogram of Gaussian 98 was used to generate molecular electrostatic potential (MEP) surfaces, which are visualized using Molekel 4.0. The transition-state structures of PfADA, HsADA, and BtADA are also displayed as stick models (the bottom structures). The ribosyl moieties were replaced with a methyl group for both the modeling and structural illustrations.

overall transition-state structures is subject to the accuracy of KIEs, commitment factors, and computational theory. The best solutions to the transition states were triangulated by matching [1-^{15}N], [6-^{13}C], and [6-^{15}N] KIEs exactly.[38] All three transition states show similarity to the Meisenheimer intermediate. Natural bond orbital analysis was performed on the optimized structures by using the POP = NBO option in Gaussian 98. Pauling bond orders of [N1−H] in the transition states were calculated on the basis of the equation ($r_n = r_1 - 0.3 \ln n$) described previously,[39] and the bond length of 1.01 Å was used for a fully formed N−H bond.

Calculations of Molecular Electrostatic Potential Surfaces. The CUBE subprogram of Gaussian 98 was used for calculating molecular electrostatic potential (MEP) surfaces of adenosine, the Meisenheimer intermediate, inosine, coformycin, and the transition-state structures. The formatted checkpoint files used in the CUBE subprogram were generated by geometry optimization at the B3LYP/6-31G (d, p) level. The MEP surfaces were visualized using Molekel 4.0 at a density of 0.1 electron/Å^3.

Scheme 1 [a]

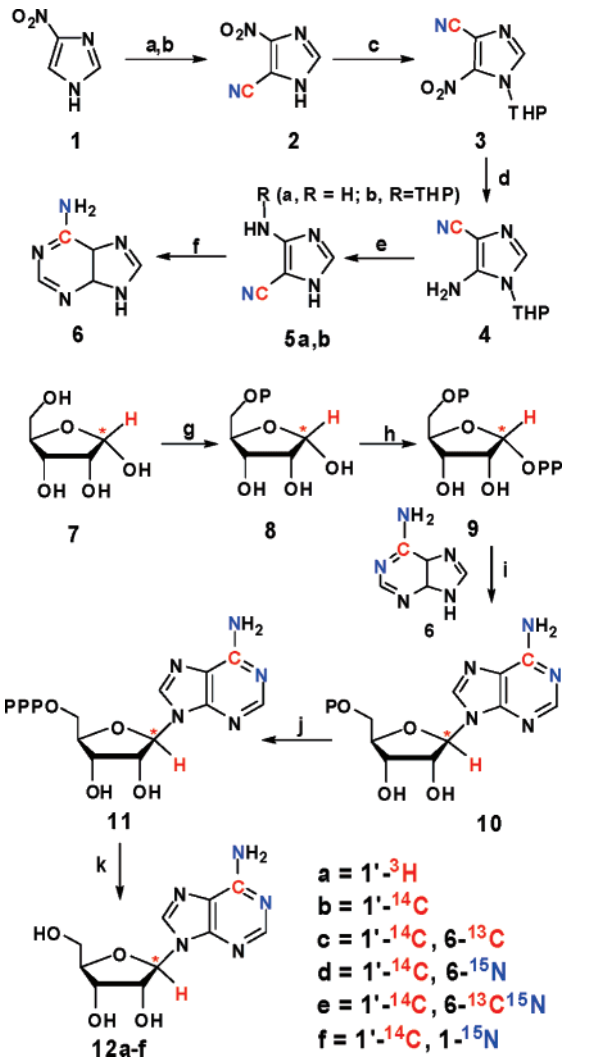

[a] Reagents and conditions: (a) HNO_3, Ac_2O; (b) K*CN* (*^{13}CN*, C*^{15}N*, or *^{13}C^{15}N*), $NaHCO_3$, MeOH, H_2O (58−62%); (c) DHP, *p*-TsOH, EtOAc; (d) 1 atm of H_2, Raney Ni, H_2O−EtOH (5:95); (e) TFA, MeOH (2:5); (f) formamidine acetate, TEA, 2-ethoxyethanol; (g) adenosine triphosphate (ATP), ribokinase (RK); (h) ATP, 5-phospho-D-ribosyl-1-pyrophosphate (PRPP) synthase; (i) adenine phosphoribosyltransferase (APRTase); (j) phosphoenolpyruvate, adenylate kinase (AK), and pyruvate kinase (PK); (k) glucose, hexokinase (HK), adenylate kinase, and alkaline phosphatase.

Results and Discussion

Synthesis of [6-^{13}C]-, [6-^{15}N]-, [1-^{15}N]-, [1′-^{3}H]-, and [1′-^{14}C]Adenosines. Scheme 1 indicates the synthetic routes to isotopically labeled adenosines **12a**−**f**. 4-Nitroimidazole (**1**) was nitrated at N3 to yield 1,4-dinitroimidazole.[34] ^{13}C-, ^{15}N-, or ^{13}C^{15}N-labeled 5-nitroimidazole-4-carbonitriles **2** were prepared through a *cine* nucleophilic substitution of 1,4-dinitroimidazole with corresponding isotopically labeled potassium cyanides.[35] The N−H of **2** was protected with dihydropyran to give THP-derivative **3** as a single regioisomer.[35] This precursor was converted to 5-amino-1*H*-imidazole-4-carbonitrile (**5**) via Raney

(38) Among KIEs, commitment factors, and computational theory, the uncertainties of the ADA transition states are largely caused by the errors of measured KIEs. Commitment factors for all the three ADAs are close to zero and therefore do not contribute to the errors in the intrinsic KIEs. In addition, the small magnitudes of KIEs are not sensitive to the errors of commitment factors. The density functional methods are fairly accurate in calculating KIEs,[24] and thus, the computational errors are mainly due to uncertainty of vibrational scaling factor for frequency calculation. However, the optimization and frequency calculation for both substrate and transition states were performed at the same level of theory and basis sets; therefore, this approach cancels out uncertainty of scaling factors. The errors in intrinsic KIEs are in third decimal points for all KIEs, which correspond to bond lengths of less than 0.1 Å when translated to the transition state geometry. The transition-state structures were obtained by exactly matching KIEs in third decimal points. In addition, the four sets of KIEs ([1-^{15}N], [6-^{13}C], [6-^{15}N], and [6-^{13}C, 6-^{15}N]) further triangulated transition state to a single structure with a bond-length fluctuation of less than 0.2 Å (95% confidential level).

(39) Mentch, F.; Parkin, D. W.; Schramm, V. L. *Biochemistry* **1987**, *26*, 921−930.

Table 1. Intrinsic KIEs[a] vs Computational EIEs[b] of PfADA, HsADA, and BtADA

adenosine pairs[c]	type of KIEs	intrinsic KIEs ^{13}k, ^{15}k, $^{13,15}k$, and ^{3}k vs computational EIEs[d,e] PfADA	HsADA	BtADA
[1-^{15}N, 1-^{14}C] vs [1-^{3}H]	β-secondary ^{15}N	1.009 ± 0.003 (1.009)	1.002 ± 0.003 (1.003)	0.995 ± 0.003 (0.994)
[6-^{13}C, 1-^{14}C] vs [1-^{3}H]	α-primary ^{13}C	1.010 ± 0.004 (1.010)	1.005 ± 0.004 (1.005)	1.004 ± 0.004 (1.005)
[6--^{15}N, 1-^{14}C] vs [1-^{3}H]	α-primary ^{15}N	1.011 ± 0.004 (1.011)	1.005 ± 0.003 (1.005)	1.001 ± 0.004 (1.001)
[6-^{13}C, 6-^{15}N, 1-^{14}C] vs [1-^{3}H]	α-primary ^{13}C^{15}N	1.021 ± 0.005 (1.021)	1.006 ± 0.005 (1.010)	1.006 ± 0.004 (1.006)
^{13}C^{15}N calcd[f]	α-primary ^{13}C^{15}N	1.021 ± 0.005	1.010 ± 0.006	1.005 ± 0.005
[1-^{14}C] vs [1-^{3}H]	remote ^{3}H[g]	1.012 ± 0.002	1.006 ± 0.001	1.000 ± 0.002

[a] Intrinsic KIEs ^{13}k, ^{15}k, and $^{13,15}k$ of PfADA, HsADA, and BtADA were obtained after correcting the remote [1′-^{3}H] KIE and the commitment factors. [b] Computational EIEs were calculated from the frequencies of the substrate and the transition states using ISOEFF98 program.[37] [c] Isotopically labeled positions are indicated. [d] At least 5 measurements were made for each experimental KIE, and standard errors are calculated from the variation between experiments. [e] Values are the intrinsic KIEs ^{13}k, ^{15}k, $^{13,15}k$, and ^{3}k with their standard deviations. The numbers in parentheses are the corresponding computational EIEs. [f] Calculated from the product of [6-^{13}C] and [6-^{15}N] KIEs. [g] This remote ^{3}H KIE arises from ^{3}H hyperconjugation with purine ring as discussed in the text.

Ni hydrogenation, followed by TFA-facililated deprotection. One-step conversion from **2** to **5** could not be achieved by either palladium−carbon or Raney Ni-catalyzed hydrogen reduction. The last step of synthesizing [6-^{13}C]-, [6-^{15}N]-, and [6-^{13}C, 6-^{15}N]adenines **6** was accomplished by ring closure of **5** using formamidine (95% for this step and 92% from **2**). We noticed that intermediate **5** is a mixture containing 9:1 **5a**,**b**. However, this mixture was not subject to further purification because the THP group of **5b** was readily removed under the condition of the subsequent cyclization step.

Adenine and its [6-^{13}C], [6-^{15}N], [6-^{13}C, 6-^{15}N] (**6** in Scheme 1), and [1-^{15}N][30] isotopic isomers were combined with [1-^{3}H]- or [1-^{14}C]riboses to give adenosines with overall yield above 98% (**7** to **12a**−**f** in Scheme 1). Briefly, the 5-hydroxyl group of [1-^{3}H]- or [1-^{14}C]riboses **7** was phosphorylated using ribokinase (RK). The subsequent labeled intermediates **8** were enzymatically converted to adenosine triphosphates **11** ([6-^{12}C/^{13}C, 6-^{14}N/^{15}N]-, [1-^{14}N/^{15}N]-, and [1′-^{3}H/^{14}C]ATP in a one-pot reaction from **7** to **11**).[33] Isotopically labeled adenosines **12a**−**f** were obtained through three dephosphoration steps of **11** using hexokinase, adenylate kinase, and alkaline phosphatase (a one-pot reaction from **11**).[31]

In comparison to previous reports of adenine synthesis,[30,40] our synthesis (**1** to **6** in Scheme 1) features an efficient approach to 6-isotopically labeled adenines for both quantitative yields and simple purification steps (see Experimental Section). The same strategy is also applicable to 1-, 2-, 3-, or 6-isotopically labeled adenines and their ribosyl derivatives by using the appropriate isotopic precursors. For instance, [3-^{15}N]- and [2-^{13}C]adenines can be prepared from [4-^{15}N]nitroimidazole and ^{13}C-formamidine, respectively. High yields, simple purification, and one-pot enzymatic reactions featured in Scheme 1 also make this approach suitable to microscale synthesis of radioactive adenine derivatives.

Apparent KIEs, Remote Label KIEs, and Commitment to Catalysis. We examined apparent [1-^{15}N], [6-^{13}C], and [6-^{15}N] KIEs of PfADA, HsADA, and BtADA (Table 1). Competitive KIE experiments were carried out with [1′-^{14}C] as remote label for heavy isotopic adenosines (^{15}N or ^{13}C) and [1′-^{3}H] as remote label for their light isotopic pairs. $^{13}(V_{max}/K_m)$ and $^{15}(V_{max}/K_m)$ for ^{13}C and ^{15}N KIEs were calculated by correcting the apparent [1-^{15}N], [6-^{13}C], and [6-^{15}N] KIEs for the remote [1′-^{3}H] KIEs,[19,25,27,28,41] which were determined with [1′-^{3}H] and [1′-^{14}C]adenosine pair (0−1.2%, Table 1). Here the [1′-^{14}C] KIE is assumed to be unity because it is four bonds away from the reaction center and ^{14}C, unlike ^{3}H (discussion below), does not generate KIEs for geometric variation around the N-ribosidic bond.[19,27]

The $^{13}(V_{max}/K_m)$ and $^{15}(V_{max}/K_m)$ KIEs obtained via the competitive experiments include the contribution of commitment factors. Large commitment to catalysis obscures experimental KIEs which must be corrected for the commitment factor according to eq 4 to give intrinsic isotope effects. Intrinsic V_{max}/K_m KIEs report on bond vibrational environment at the transition states and include equilibrium binding isotope effects prior to transition state formation.[27,28] In eq 4, $^{X}(V/K)$ is the observed heavy atom KIE, ^{X}k is the intrinsic KIE, ^{X}K is the equilibrium isotope effect between substrate and product, C_f and C_r are forward and reverse commitment, respectively, and X is the specific isotope ^{3}H, ^{13}C, or ^{15}N, respectively.

$$^{X}(V/K) = \frac{^{X}k + C_f + C_r \times {}^{X}K_{eq}}{1 + C_f + C_r} \qquad (4)$$

Forward commitments of PfADA, HsADA, and BtADA were examined by the isotope trapping method as described in the Experimental Section.[27] The forward commitment factors were $C_f = 0.006 \pm 0.001$, 0.020 ± 0.004, and 0.03 ± 0.005 for PfADA, HsADA, and BtADA (Figure 2), respectively. The small values of C_f indicate that adenosine is not a committed substrate for the three ADAs. Their Michaelis complexes convert to product at much slower rates than equilibration with unbound substrates.[17] The same conclusion has also been drawn for BtADA through a different approach.[42] The 3−5-fold decrease of C_f from HsADA and BtADA to PfADA is consistent with smaller k_{cat} values and comparable K_m values for PfADA relative to HsADA and BtADA (1.8 s^{-1} vs 36 and 65 s^{-1}; 29 μM vs 22 and 56 μM, respectively).[22,29] Reverse commitment factors C_r of the three ADAs are assumed to be zero because the ADA-catalyzed aminohydrosis reaction is experimentally irreversible. The intrinsic KIEs (^{X}k) were therefore derived on the basis of C_f and $C_r = 0$. Due to zero C_r and negligible C_f, the experimentally measured apparent KIEs of PfADA, HsADA, and BtADA are within experimental error of the intrinsic KIEs.

Computational Modeling of Transition States for PfADA, HsADA, and BtADA. The intrinsic [1-^{15}N], [6-^{13}C], [6-^{15}N],

(40) Barrio, M. D.; Scopes, D. I.; Holtwick, J. B.; Leonard, N. J. *Proc. Natl. Acad. Sci. U.S.A.* **1981**, *78*, 3986−3988.
(41) Birck, M. R.; Schramm, V. L. *J. Am. Chem. Soc.* **2004**, *126*, 6882−6883.
(42) Weiss, P. M.; Cook, P. F.; Hermes, J. D.; Cleland, W. W. *Biochemistry* **1987**, *26*, 7378−7384.

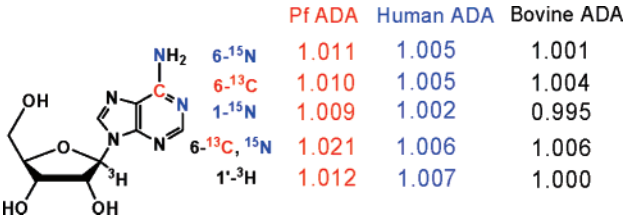

Figure 4. Intrinsic KIEs for the deamination reactions catalyzed by PfADA, HsADA, and BtADA. The structure of adenosine is shown with a summary of the KIE values (see Table 1 for details).

and [6-^{13}C, 6-^{15}N] KIEs (^{13}k, ^{15}k, and $^{13,15}k$) of PfADA, HsADA, and BtADA were derived from the corresponding apparent KIEs upon correction of the remote [1′-^{3}H] KIEs and commitment factors as discussed above (Table 1). The KIEs provide boundary conditions for solving the transition-state structures.[19,27,28] The transition-state calculations for PfADA, HsADA, and BtADA used 9-methyladenine as a substrate mimic and a hydroxyl anion as the nucleophile. The B3LYP functional and the 6-31G (d, p) basis set were used to optimize and calculate the vibrational frequencies of the transition states and the substrate.

The transition-state structures of the three ADAs that give the best match to the intrinsic [1-^{15}N], [6-^{13}C], and [6-^{15}N] KIEs feature Meisenheimer intermediate-like geometry with significant sp^3 hybridization at C6 and distinct partial N1-protonation states (Figures 3 and 4 and Table 1). Adenosine deaminations are aromatic nucleophilic substitutions that form Meisenheimer complexes followed by NH_2-6 protonation and elimination as proposed for yeast AMP deaminase and mouse ADA.[3,31,43] The Meisenheimer intermediate is characterized by complete protonation at N1 and sp^3 hybridization at C6 with full [N−H], [C6−O^{hydroxyl}], and [C6−N6] bond orders (Figure 1). Computational analysis of intrinsic KIE indicates that the evolution of the transition states for PfADA, HsADA, and BtADA are completed prior to the formation of the Meisenheimer complex. This conclusion comes from the correlation of calculated KIEs to intrinsic KIEs. Small normal to slightly inverse [1-^{15}N] intrinsic KIEs of 1.009 to 0.995 correspond to partially protonated N1s at the transition state. In contrast, a large inverse KIE of 0.983 was calculated for full N1-protonation at the transition state (see discussion below). The small but normal [6-^{15}N] KIEs of 0.1−1.1% are consistent with an insignificant dissociation of the C6−N6 bond and no protonation of the 6-exocyclic amine at the transition states. Large inverse [6-^{15}N] KIEs would be expected for bonded N6-ammonium ($-NH_3^+$) ion at the transition state.[31] Consequently, these [6-^{15}N] KIEs provide evidence to support transition state formation prior to the Meisenheimer intermediate. The small primary [6-^{13}C] intrinsic KIEs (1.001, 1.004, and 1.010 for PfADA, HsADA, and BtADA, respectively) are generated in the transition states by significant C6-sp^3 hybridization (sp$^{2.95\ to\ 3.04}$) and nearly full bond orders of C6−N6 and C6−O^{hydroxyl} (Table 2).

Remote [1′-^{3}H] KIEs. The tritium of [1′-^{3}H]adenosine is four bonds away from the reaction center and is not expected to be influenced by the chemistry at the reaction center (C6).[27,41] However, a remote ^{3}H substitution is sensitive to geometrical distortion and can report KIEs as large as 6.0% stemming from the difference in N-ribosidic tortion angles between unbound substrate and enzyme-bound transition states.[19,25,28,41] The remote [1′-^{3}H] KIEs of the three ADAs are 1.012 for PfADA, 1.007 for HsADA, and unity for BtADA (Table 1 and Figure 4). The significant [1′-^{3}H] KIEs in the case of PfADA and HsADA indicate that the O4′−C1′−N9−C8 torsional angle is altered at their transition states relative to unbound substrate for which the O4′−C1′−N9−C8 torsional angle is expected to adopt multiple orientations as the barrier for rotation is small (less than 0.8 kcal/mol).[24,25] The restriction of rotation around the C1′−N9 glycosidic bond can alter the hyperconjugation between the π system in the purine ring and the σ^* (C1′−H1′) orbital and thereby weaken the C1′−H1′ σ bond at the bound transition state relative to free substrate. This geometrical preference can cause an equilibrium isotope effect up to 1.08.[24,25,27] In addition, strain between the purine and ribosyl groups can also cause an isotope effect by distortion of the sp^3 geometry at C1′.[44,45] The significant [1′-^{3}H] KIEs of PfADA and HsADA indicate that the $\pi-\sigma^*$ interaction or the sp^3 distortion at their transition states is different from that of BtADA. Although the O4′−C1′−N9−C8 torsion angles in these cases have not been determined, these torsion angles among the three transition states are expected to be within 20 deg of each other on the basis of the small difference of their [1′-^{3}H] KIEs (1.000−1.012).[24,25]

Table 2. Representative Geometric and Electronic Changes of the Substrate and the Transition States for PfADA, HsADA, and BtADA Calculated Using B3LYP/6-31G(d,p) in Gaussian 98

		transition state		
param	substrate[a]	PfADA	HsADA	BtADA
Bond Length (Å)				
C6−N6	1.356	1.510	1.461	1.420
C6−O^{hydroxyl}	NA	1.391	1.440	1.504
N1−H	NA	1.915	1.550	1.275
Hybridization				
C6 (in C6−N1 bond)[b]	sp$^{2.29}$	sp$^{2.95}$	sp$^{3.02}$	sp$^{3.04}$
N1 (in C6−N1 bond)	sp$^{1.89}$	sp$^{1.55}$	sp$^{1.43}$	sp$^{1.45}$
Bond Order[c]				
C6−N6	0.985	0.959	0.966	0.970
C6−O^{hydroxyl}	NA	0.946	0.938	0.924
N1−H[d]	NA	0.05	0.16	0.42
σ Occupancy				
C6−N6	1.991 88	1.983 71	1.986 48	1.987 96
C6−O^{hydroxyl}	NA	1.988 49	1.987 48	1.984 43
σ^* Occupancy				
C6−N6	0.030 65	0.064 78	0.055 20	0.0474 1
C6−O^{hydroxyl}	N.A.	0.095 42	0.112 25	0.135 90
Charge[e]				
C6	+0.431	+0.586	+0.587	+0.583
N6	−0.821	−0.912	−0.922	−0.925
N1	−0.558	−0.466	−0.571	−0.646

[a] The ribosyl moieties of the substrate and the transition states were replaced with a methyl group. [b] The rehybridization of C6 in the C6−N1 bond. [c] Calculated by subtracting the number of electrons occupying the σ^* orbital from the number occupying the σ orbital divided by a factor of 2. The bond order of 1 means two electrons in the σ-bonding orbital and no electron in the antibonding orbital. [d] Pauling bond orders of [N1−H] in the transition states were calculated on the basis of the equation ($r_n = r_1 - 0.3 \ln n$) described previously,[39] and the bond length of 1.01 Å was used for a fully formed N−H bond. [e] Natural charges are shown.

β-Secondary [1-^{15}N] KIEs. The β-secondary [1-^{15}N] intrinsic KIEs of 1.009, 1.002, and 0.995 were measured for PfADA, HsADA, and BtADA, respectively (Table 1 and Figure 4). The

(43) Sharff, A. J.; Wilson, D. K.; Chang, Z.; Quiocho, F. A. *J. Mol. Biol.* **1992**, *226*, 917−921.
(44) Horenstein, B. A.; Parkin, D. W.; Estupinan, B.; Schramm, V. L. *Biochemistry* **1991**, *30*, 10788−10795.
(45) Horenstein, B. A.; Schramm, V. L. *Biochemistry* **1993**, *32*, 7089−7097.

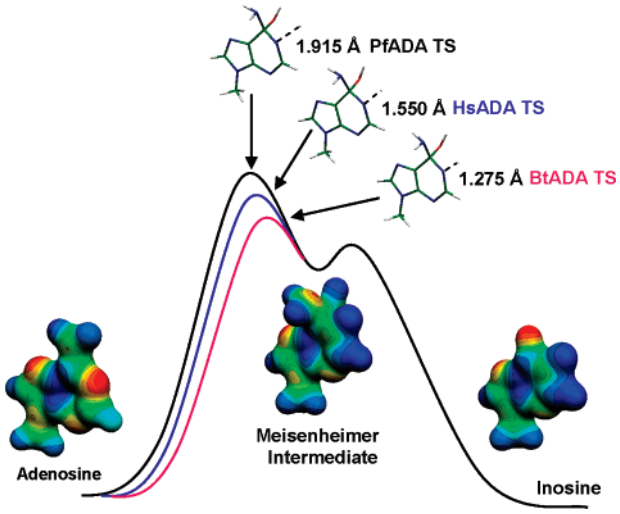

Figure 5. Reaction coordinates for adenosine deamination catalyzed by PfADA, HsADA, and BtADA. The relative energy along the reaction coordinate is arbitrary with the highest energetic points as the transition states. The second transition state represents protonation and loss of the exocyclic amino group. The transition state analysis provides no information for the intermediate and following step except that its energetic barrier is low relative to formation of the Meisenheimer intermediate.

β-secondary [1-^{15}N] KIE reports on the protonation state of N1 and also on the [C6−N1] bond order at the transition state. The calculation predicts a 1-^{15}N KIE of 0.983 for a transition state that resembles the Meisenheimer intermediate that is fully protonated at N1. A similar inverse KIE of 0.988 was reported for the protonation and rehybridization of the pyrimidine N3 in cytidine deaminase-catalyzed aminohydrolysis.[46] The slight inverse to normal [1-^{15}N] KIEs of 0.995−1.009 for PfADA, HsADA, and BtADA therefore indicated that these enzymes have partially protonated N1s at their transition states. The magnitude of the [1-^{15}N] KIEs, 1.009 for PfADA, 1.002 for HsADA, and 0.995 for BtADA, is reflected in the optimized transition-state structures. These isotope effects correspond to increased N1−H Pauling bond orders of 0.05, 0.16, and 0.42[39] with decreased N1−H bond lengths of 1.915, 1.550, and 1.275 Å, respectively (Table 2). Partial protonation of N1 also correlates with the increase in s-orbital character of N1 in the C6−N1 bond from sp^2 in the substrate to sp$^{1.43-1.55}$ in the transition states (Table 2). The variable and partial protonation of N1 indicates that the transition states of PfADA, HsADA, and BtADA are formed prior to the formation of the Meisenheimer intermediate. The transition-state structures of PfADA, HsADA, and BtADA are different from that of yeast AMP deaminase, where the N1 is fully protonated at the transition state.[31] The altered N1−H bond orders at these transition states indicate that PfADA has the earliest and BtADA has the most developed transition state on the path to the covalent Meisenheimer intermediate (Figure 5).

α-Primary [6-^{15}N] KIEs. In adenosine deamination, the [6-NH$_2$] group experiences loss of conjugation from the purine ring as C6 becomes more sp^3-like at the transition state. C6−N6 bond order is lost as a result of this rehybridization. Generation of Meisenheimer complex is followed by [6-NH$_2$] protonation and subsequent departure to form inosine. Small normal or slightly inverse [1-^{15}N] KIEs in PfADA, HsADA, and BtADA (discussed above) indicate that the ADA transition states occur before formation of the Meisenheimer complex. Small, normal primary [6-^{15}N] KIEs of 0.1−1.1% for the three ADAs (Table 1 and Figure 4) can be attributed to the change of the [C6−N6] bond order following hydroxide attack and the subsequent C6-sp^3 rehybridization. The 6-^{15}N KIE of BtADA 1.001 reported here is consistent with the KIE of 1.004, which was reported earlier by measuring the natural abundance of ^{15}N via isotope ratio mass spectrometric analysis.[42] The normal primary [6-^{15}N] KIEs rule out late transition states involving protonation of 6-NH$_2$. This mechanism would cause a large inverse KIE.[31] The transition states modeled by correlating the calculated EIEs to the intrinsic KIEs show longer C6−N6 bond distances (1.420−1.501 Å) compared to the substrate (1.356 Å in Table 2). The primary [6-^{15}N] KIEs of 1.011 for PfADA, 1.005 for HsADA, and 1.001 for BtADA are consistent with C6−N6 bond orders of 0.959, 0.966, and 0.970, respectively, with the C6−N6 bond lengths of 1.501, 1.461, and 1.420 Å for PfADA, HsADA, and BtADA, respectively (Table 2).

α-Primary [6-^{13}C] and [6-^{13}C, 6-^{15}N] KIEs. Primary [6-^{13}C] KIEs for PfADA, HsADA, and BtADA are influenced by the change in bond order to the leaving group, participation of the hydroxyl nucleophile, and N1 protonation at the transition state. The hybridization of C6 is sp^3-like at the transition state due to the nucleophilic addition of the Zn^{2+}-activated hydroxide. The newly formed C6−O^{hydroxyl} bond increases the overall bond order at C6 and causes a 6-^{13}C KIE. The calculations show that hydroxyl attack is nearly complete at the transition states with bond orders of 0.946, 0.938, and 0.924 for PfADA, HsADA, and BtADA, respectively (Table 2). The corresponding C6−hydroxide oxygen bond distances are 1.391, 1.440, and 1.504 Å, respectively, close to the fully developed C6−O^{hydroxyl} σ bonds. In contrast, the sp^3 hybridization of C6 at the transition state and the protonation of N1[43,46,47] weaken the [C6−N6] and [C6−N1] bonds. These destabilizing effects are reflected as decreased C6−N6 bond distances and the smaller C6−N1 s-orbital hybridization (Table 2) compared to the substrate (1.420−1.501 Å vs 1.356 Å and sp$^{1.43-1.55}$ vs sp$^{1.89}$, respectively). For the three ADAs, the total bond orders of C6 remain relatively unchanged at the transition states. The calculation results are consistent with the small primary [6-^{13}C] KIEs of 1.004−1.01 for PfADA, HsADA, and BtADA (Table 1 and Figure 4). These results differ from the large primary [6-^{14}C] KIE of 1.042 for yeast AMP deaminase, where the C6−O^{hydroxyl} bond at the transition state has a bond order of 0.80, and C6 is involved in reaction coordinate motion.[31]

The [6-^{13}C] and [6-^{15}N] KIEs of the three ADAs (primary ^{13}k and ^{15}k in Table 1) are small and thus might be sensitive to experimental errors. To further validate the intrinsic [6-^{13}C] and [6-^{15}N] KIEs above, we determined primary [6-^{13}C, 6-^{15}N] KIEs ($^{13,15}k$) for PfADA, HsADA, and BtADA using [6-^{13}C, 6-^{15}N]-double-labeled substrate with [1′-^{14}C] as the remote label. The $^{13,15}k$ KIEs showed good agreement with the products of the corresponding primary KIEs of ^{13}k and ^{15}k (Table 1). This consistency confirms the intrinsic [6-^{13}C] and [6-^{15}N] KIEs and supports their use in establishing transition-state structures. Comparison of [6-^{13}C] and [6-^{15}N] KIEs with the combined effect also establishes that the KIEs occur on the same chemical step—the formation of the Meisenheimer complex.

(46) Snider, M. J.; Reinhardt, L.; Wolfenden, R.; Cleland, W. W. *Biochemistry* **2002**, *41*, 415−421.

(47) Wilson, D. K.; Quiocho, F. A. *Biochemistry* **1993**, *32*, 1689−1694.

Molecular Electrostatic Potential Comparison of Substrate, Transition States, and Coformycin. Molecular electrostatic potential surfaces (MEP) reflect the bond geometry and electron distribution of defined molecules and are useful for probing evolution along the reaction coordinate.[25,27] The MEP profiles of PfADA-, HsADA-, and BtADA-catalyzed deamination reactions reveal that their transition states resemble the Meisenheimer intermediate complex rather than the substrate or the product (Figure 3). The hydroxyl attack and sp^3 rehybridization at C6 make the N6 electrostatic potential more negative in the transition states with overall charges of −0.912 to −0.925. In contrast, the NH_2 of adenosine has a total charge of −0.821 (Table 2). The protonation of N1 converts the negative electrostatic potential of N1 to a positive MEP of NH at the transition states.

The transition-state structures of PfADA, HsADA, and BtADA show slight differences in the [C6−$O^{hydroxyl}$], [C6−N6], and [C1−N1] bond orders and therefore the corresponding bond distances (Table 2). The key variation among the three ADA transition states lies in the degree of their distinct N1 protonation. This difference is reflected in the MEPs of the transition states with electron density expanded at N1 due to its protonation. The relatively high Pauling bond order of [N1−H] makes the transition state of BtADA more like a Meisenheimer intermediate than those of PfADA and HsADA (Figure 3). The overall structures of the three ADA transition states are similar to Meisenheimer intermediate rather than the reactant adenosine and the product inosine. This observation is consistent with Jencks' whimsical description of "Bema Hapothle" (Bell−Marcus−Hammond−Polanyi−Thornton−Leffler) transition-state theory,[48] which proposes that the transition state most similar to the intermediate will be the most reactive. *R*-Coformycin (Figure 1) is a picomolar inhibitor of adenosine deaminases.[10,22] The *R*-hydroxyl of this molecule mimics the attacking hydroxyl, and the unconjugated 7-membered ring mimics the protonated N1 at the transition states. Consequently, the overall MEP of *R*-coformycin resembles those of the Meisenheimer intermediates and the transition states of the three ADAs.

Mechanisms, k_{cat}, and Coformycin Inhibition. The reaction coordinate profiles of PfADA, HsADA, and BtADA are shown in Figure 5. The intrinsic KIEs and computational modeling results are consistent with early transition states, for which N1 is partially protonated and the hydroxyl attack is nearly complete. These transition states are at highest energetic barrier on the path to the formation of Meisenheimer intermediate. The protonation of NH_2-6 and its loss are sufficiently fast to give the product in the steps past the rate-limiting formation of the Meisenheimer intermediate. The deamination mechanisms of PfADA, HsADA, and BtADA are different from that of *Escherichia coli* cytidine deaminase, where a stepwise mechanism with a relatively rapid formation of the Meisenheimer intermediate is followed by rate-determining ammonia elimination.[46] The transition states of the three ADAs are also distinct from that of yeast AMP deaminase, where the transition state is characterized by a partial hydroxyl attack with a bond order of 0.8 and complete N1 protonation.[31]

Of the three transition states, PfADA has the earliest and BtADA has the most developed transition state with HsADA somewhere between. These different transition-state structures are reflected by variation in the N1−H bond distances. The change of the total energy computed for the three transition states shows the same pattern with the lowest for BtADA, followed by a 2.4 kcal/mol increase for HsADA and another 1.3 kcal/mol increase for PfADA (Supporting Information). Consequently, the extent of N1 protonation is a key step in forming the transition states. The distinct N1 protonation between HsADA and BtADA transition states is remarkable because their amino acid sequences are 91% homologous and their active sites are completely identical.[6] A glutamic acid in murine ADA (E217),[3,43] BtADA (E214),[6] and HsADA (E217)[49] has been identified as the residue for N1 protonation, and an E217A mutation causes HsADA to be inactive.[49] The E200 of PfADA[10] is expected to play the same role on the basis of sequence alignment. We can postulate that the dynamic vibrational range of BtADA E214 might account for formation of the most Meisenheimer intermediate-like transition state. The most developed N1 protonation corresponds to the most Meisenheimer intermediate-like transition state, and the lowest energetic barrier to transition state formation. Differences in the total energy for PfADA, HsADA, and BtADA transition states (Figure 5 and discussion above) correspond to the observed 36-fold (2 kcal/mol) enhancement of k_{cat} in PfADA, HsADA, and BtADA (1.8, 36, and 65 s^{-1}, respectively).[22] The value of 2 kcal/mol is slightly smaller than the total energy difference (3.7 kcal/mol) computed for the three transition states (results above) and might be accounted by the subtle species-dependent energetic differences for PfADA, HsADA, and BtADA.

A perfect transition state analogue inhibitor can achieve dissociation constants as low as 10^{-13} to 10^{-25} M.[17] *R*-Coformycin (Figure 1) is a transition-state analogue inhibitor and inhibits PfADA, HsADA, and BtADA with dissociation constants of 60, 100, and 80 pM, respectively.[10,22] The transition-state structures of PfADA, HsADA, and BtADA are similar to the Meisenheimer intermediate and *R*-coformycin by comparing their MEPs (Figure 3). The tight binding of *R*-coformycin and deoxycoformycin with adenosine deaminases support this similarity. However, the purine ring of the three ADA transition states (see the bond distances in Table 2) is smaller than the 7-member-ring of *R*-coformycin. In addition, the unsaturated 7-member-ring of coformycin is less planar around the *R*-hydroxyl group when compared to the 6-member-ring of the three transition states (Figure 3). *R*-Coformycin is fully protonated at the N corresponding to the partial N1 protonation of PfADA, HsADA, and BtADA transition-state structures. These differences may explain the less than optimal affinity of *R*-coformycin compared with an ideal transition state mimic.

Conclusion

Labeled adenines were synthesized via an efficient new approach, which provides excellent yields, ready purification, and versatility for atomic labeling. Labeled adenines were enzymatically coupled to isotopically labeled ribosyl groups to give local and remote labeled adenosines. Labeled ADA substrates were used to examine the KIEs of PfADA, HsADA, and BtADA. The intrinsic KIEs were matched to density functional calculations to show that the three transition states

(48) Jencks, W. P. *Chem. Rev.* **1985**, *85*, 511−527.

(49) Bhaumik, D.; Medin, J.; Gathy, K.; Coleman, M. S. *J. Biol. Chem.* **1993**, *268*, 5464−5470.

are close to the Meisenheimer intermediate but differ from one another. The key structural variation between the Meisenheimer intermediate and the three enzymatic transition states lies in their distinct partial N1 protonation states. In contrast, the attack of the Zn^{2+}-activated hydroxyl is almost complete for PfADA, HsADA, and BtADA transition states. Thus, PfADA has the earliest and BtADA has most developed transition state on the path to the covalent Meisenheimer intermediate. Protonation of NH_2-6 and subsequent deamination occur rapidly after the formation of the Meisenheimer intermediate. The catalytic turnover (k_{cat}) of the enzymes corresponds to the position of the transition states prior to formation of the Meisenheimer complex. The MEPs of PfADA, HsADA, and BtADA transition states are similar to that of coformycin, a picomolar ADA inhibitor. This observation is consistent with the tight binding of coformycin to ADAs. These results are useful for probing the transition-state structures of other ADAs and for the design of transition state analogue inhibitors against other ADA isozymes.

Acknowledgment. We thank Professor Kami Kim and Dr. Li-Min Ting for providing HsADA and Dr. Sean M. Cahill for ^{15}N NMR measurement. This work was supported by NIH Grant CA724444.

Supporting Information Available: Reference S1 and complete calculation results of the transition states, adenosine, inosine, the Meisenheimer intermediate, and coformycin. This material is available free of charge via the Internet at http://pubs.acs.org.

JA072122Y